Two Distinct Types of Orientation Process Observed in Uniaxially Elongated Smectic LC Melt

Kensuke Osada,† Masao Koike, Hirotaka Tagawa, Shin-ichiro Hunaoka, Masatoshi Tokita, and Junji Watanabe*

Department of Organic and Polymeric Materials, Tokyo Institute of Technology, Ookayama, Meguro-ku, Tokyo 152-0033, Japan

Received March 29, 2005; Revised Manuscript Received June 19, 2005

ABSTRACT: We examine the tensile deformation of the smectic melt of a main-chain liquid crystalline polymer. A film molded in isotropic melt is heated to a smectic temperature of 60 °C and then stretched at selected strain rates. In the initial stage of strain below 100% (defined as $\{(l - l_0)/l_0\} \times 100\%$), smectic layers align parallel to the stretching direction; i.e., polymer chains orient perpendicularly (so-called "perpendicular orientation"). This perpendicular orientation in the low-strain region is invariably observed at any strain rate. Upon succeeding elongation, however, two distinct types of orientation process are observed depending on the strain rate. On elongation at strain rates as low as 5%/min, the perpendicular orientation is improved until the sample breaks at 400% strain (process A). At a high strain rate of 100%/min, in contrast, the perpendicular orientation initially observed is eventually altered to the "parallel orientation" with polymer chains lying parallel to the tensile axis (process B). In this case, the well-known necking takes place, and the sample breaks at an extremely large strain more than 3000%. These two distinct elongation processes are also dependent on temperature; processes A and B are observed in higher and lower temperature regions, respectively. On the basis of these data, the molecular orientation mechanisms in smectic field are discussed by coupling together the nature of smectic liquid crystal and dynamics of polymer chains.

Introduction

Chain conformation is significant subject to understand the micro- and macroscopic characteristics of liquid crystals in main-chain types of polymer. It should be decided by the interplay between the long-range orientational and positional orders of liquid crystals (LCs), which force the chain to extend over the entire chain length, and the polymeric tendency to maximize entropy, which favors conformational freedom. de Gennes first pointed out the importance of this interplay, showing that a semiflexible long chain in a nematic phase may recover some part of the entropy loss due to the ordering of mesogenic units, by forming hairpin foldings where the chain executes a counter reversal (180°) with respect to the *n*-director.[1] The statistics and dynamics of hairpins in wormlike chains have been developed by Warner and co-workers.[2,3] From small-angle neutron scattering observation, in fact, it is found that each polymer chain includes one or two hairpin foldings in the nematic orientational field.[4,5]

We are also concerned with this interplay and treating the smectic phase of main-chain BB-*n* polyesters. Our results suggest the existence of the chain-folded lamellae. The first implication was constructed from the fact that small-angle X-ray scattering (SAXS) maxima attributed to the stacked chain folded lamellae are well observed in the BB-*n* polyesters crystallized from smectic melt.[6−10] The scattering spots appear along the smectic layer normal, and their spacing is in the range of 220−300 Å, which corresponds to a length of 12−16 repeating units. It is interesting to note that the spacing decreases with an increase in crystallization temperature. This trend is opposite to that generally observed for conventional polymer crystals, suggesting that the chain-folded lamellae exist already in the preceding smectic phase as an entropic effect and their folding length is maintained on the crystallization.[8]

The lamellar structure was also suggested from the unusual orientation of polymer molecules in spun fibers.[11,12] When the fiber of BB-*n* is spun from the smectic melt, the smectic layers arrange parallel to the fiber axis; i.e., the polymer chains lie perpendicular to the fiber axis. Noticeable is that even at ambient temperature just around the glass transition temperature, the oriented fiber can be further elongated to twice its length without changing its orientation. This unusual orientation has been explained to result from the mutual sliding of the chain-folded lamellae.

The shear deformation induced by a cone−plate-type rheometer gave decisive evidence of the existence of chain-folded lamellae.[13] In the sheared smectic melt, the smectic layers align with the layer normal perpendicular to the shear direction and parallel to the velocity gradient direction. This characteristic shear flow indicates that the orientation is achieved by the slip between lamellae as in the block copolymer with the lamellar microsegregation.[14] The synchrotron radiation SAXS, in fact, exhibits a scattering maximum corresponding to the lamellar thickness of 80 Å,[13] which is ∼5 times larger than the repeating unit length.

The rheological experiment offered us further interesting information that two types of orientation are produced depending on temperature. One is the above-mentioned orientation, which is observed at lower

† Present address: Department of Materials Science and Engineering, Graduate School of Engineering, The University of Tokyo, Hongo 7-3-1, Bunkyo, Tokyo 113-8655, Japan. Ph +81-3-5841-7145, Fax +81-3-5841-7139, e-mail osada@bmw.t.u-tokyo.ac.jp.

* To whom correspondence should be addressed: Ph +81-3-5734-2633; Fax +81-3-5734-2888; e-mail jwatanab@polymer.titech.ac.jp.

10.1021/ma050649u CCC: $30.25
Published on Web 07/22/2005

smectic temperatures. In another orientation observed at higher temperatures, the smectic layers arrange with the layer normal perpendicular to both the shear and velocity gradient directions. The latter orientation results from the liquidlike packing of the mesogens within a smectic layer, since the shear gradient causes the two-dimensional liquid flow of mesogens along the layer rather than the sliding of lamellae as temperature increases. Thus, we concluded that there are two types of shear flow mechanism, which are able to produce the perpendicular orientation in the smectic melt of main-chain polymers.

In this study, a simple uniaxial elongation was applied on the smectic melt of BB-5(3-Me) polyester, and the deformation mechanisms were examined macroscopically by mechanical measurements and microscopically by X-ray measurements. Depending on both the deformation rate and temperature, two types of unique orientation processes were observed here. The appearance of these two processes is discussed by coupling the polymeric and the smectic mesophase characteristics.

Experimental Section

The BB-5(3-Me) polyester

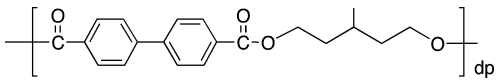

was synthesized by melt transesterification from dimethyl *p,p′*-bibenzoate and 3-methyl-1,5-pentamethylenediol with isopropyl titanate as catalyst.[15] The inherent viscosity of BB-5(3-Me), h_{inh}, is 0.72 dL/g as measured at 30 °C using 0.5 g/dL solutions in a 60/40 w/w mixture of phenol and tetrachloroethane. Molecular weight and molecular weight distribution were determined as $M_n = 53\,000$ and $M_w/M_n = 2.1$ from the GPC curve which was calibrated with a polystyrene standard.

Differential scanning calorimetric (DSC) measurement was carried out with a Perkin-Elmer Pyris I at a scanning rate of 10 °C/min under dry nitrogen flow. Wide-angle X-ray diffraction (WAXD) was recorded on the imaging plate using a Rigaku-Denki RU-200 BH with Ni-filtered Cu Kα radiation.

Film samples for mechanical stretching were prepared by pressing the isotropic melt at 170 °C, held for 5 min to possess the uniform disorder, and cooled to the LC temperature at a cooling rate of 10 °C/min. Films with a thickness of 0.5 mm were cut into rectangular strips 10 mm long and 2 mm wide and clamped in a tensile testing machine. Before each elongation measurement, the samples were annealed at respective temperatures for 1 h to ensure an equilibrium LC formation. Stress−strain curves were obtained by Seiko Instrument TMA SSC5200 and Orientech Tensilon RTC-1350A. The strain (%) was defined as $\{(l - l_0)/l_0\} \times 100\%$, where l and l_0 are the strained and unstrained lengths, respectively. The stress was evaluated using an area of the initial section of film.

Results

Characteristics in Stress−Strain Curves of Smectic Melt. BB-5(3-Me) polyester forms a smectic CA (SmCA) phase where mesogenic groups are tilting to the opposite direction in every layer and the same direction in every second layer, i.e., zigzag manner.[11,12] The novel smectic phase is formed in the wide temperature range from the glass transition temperature ($T_g = 31$ °C) to the isotropization temperature ($T_i = 149$ °C).[15,16] Crystallization does not take place at all because of the packing difficulty of alkyl spacers with the methyl substitution.

The mechanical deformation processes of the smectic melt with changes in strain rate and temperature were investigated. As found in Figure 1, films are elastically stretched in the initial stage of strain and show the typical yielding when the temperature is relatively high. Table 1 lists the basic mechanical data measured at various temperatures and the following characteristics are extracted. The initial elastic modulus decreases with increasing temperature and decreasing strain rate. The strain at the yielding point is 20%−50%, and the corresponding stress decreases with increasing temperature and decreasing strain rate.

At first, we refer to the two typical types of mechanical deformation process, which are observed depending on strain rate. Parts a and b of Figure 1 show the stress−strain ($S-S$) curves observed at a low rate of

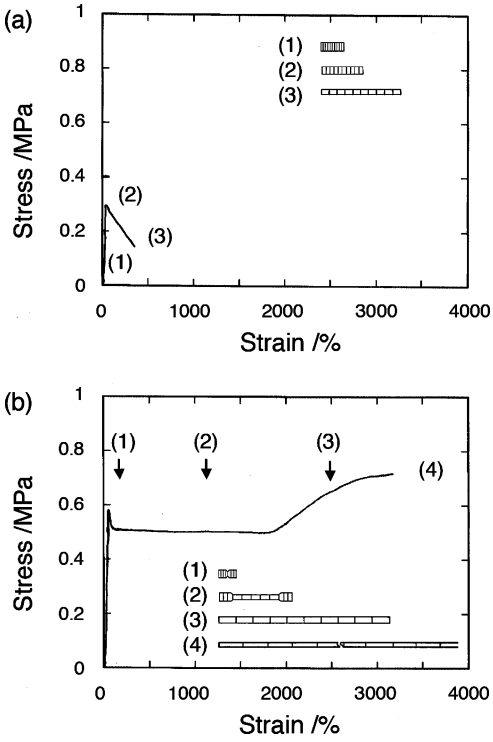

Figure 1. Stress−strain curves obtained for the smectic melt at strain rates of (a) 5%/min and (b) 100%/min. The smectic temperature is 60 °C. The shape of the film observed at each respective strain is illustrated in the inset.

Table 1. Mechanical Data Obtained from Stress−Strain Measurement

temp (°C)	strain rate (%/min)	initial elastic modulus (MPa)[a]	strain at yielding point (%)	stress at yielding point (MPa)
40	5	10.3	–	–[b]
	10	12.5	–	–
	30	12.9	–	–
	40	16.3	–	–
	50	15.0	–	–
	100	17.2	–	–
60	5	5.0	30	0.29
	30	5.9	50	0.43
	40	4.7	20	0.45
	50	5.5	25	0.5
	100	7.8	26	0.6
100	5	0.59	37	0.063
	10	0.70	20	0.064
	30	1.1	20	0.37
	40	1.1	32	0.09
	50	1.25	25	0.20
	100	1.7	35	0.30

[a] Determined at initial stage of strain where stress increases elastically with strain. [b] No clear yielding.

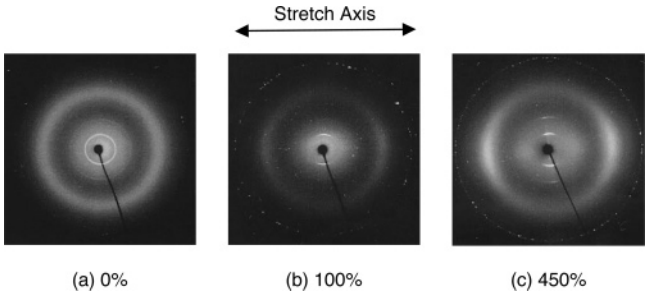

Figure 2. WAXD photographs for variously strained samples elongated at a strain rate of 5%/min at 60 °C: (a) 0%, (b) 200%, and (c) 450%. The elongation direction is horizontal.

5%/min and a high rate of 100%/min, respectively. The selected smectic temperature is 60 °C, which is 30 °C higher than T_g. The difference in $S-S$ behavior is clear between the two cases. When the film is elongated at the rate of 5%/min, the stress increases up to 0.3 MPa at around 50% strain and then decreases moderately until the film breaks at around 400% of strain. Through this deformation, the film underwent simple thinning as schematically illustrated in the inset of Figure 1a.

In contrast, the film strained at the high rate of 100%/min was found to be elongated over 3000%, which is roughly 10 times larger than that of the low-rate case. As found in Figure 1b, the yielding takes place at a similar strain of around 50% as in the low-rate case. During further elongation up to 1800% of strain, the stress stays at a constant value of 0.5 MPa. This constancy of the stress after yielding is due to the necking which can be recognized by the naked eye. The necking develops on both sides and expands over the entire length at a strain of around 1800%. The film still elongates with a uniform deformation beyond this strain and finally breaks at around 3200% strain.

The results clearly show that the deformation processes are completely different between the low-rate and high-rate cases. X-ray investigations were performed in detail focusing on the two cases of 5%/min and 100%/min.

X-ray Analyses for Deformation Process. a. Deformation Process at Low Strain Rate of 5%/min. Figure 2 shows the WAXD patterns of the films elongated at 5%/min and 60 °C. First refer to the X-ray pattern of the as-molded film in Figure 2a. It consists of two sharp inner reflections with spacings of 16.4 and 8.2 Å and broad outer halos with a spacing of 4.5 Å. The former reflections are attributable to the smectic layer order and the latter to the liquidlike packing of mesogenic groups within a smectic layer. All these reflections appear as rings, indicating no preferential orientation of molecules in the as-molded film. When the film is strained up to 200%, the layer reflections and outer haloes become concentrated in the meridian and equator, respectively, as observed in the X-ray pattern of Figure 2b where the film was stretched in the horizontal direction. Thus, the elongation forces the anomalous orientation such that the smectic layers align parallel to the tensile direction; i.e., the polymer chains lie perpendicular to the tensile direction. We call this anomalous orientation "perpendicular orientation". By further elongation, the layer reflections are concentrated more and more on the meridian (see Figure 2c). Thus, no distinct event takes place before breaking. Only the orientation of layers is improved.

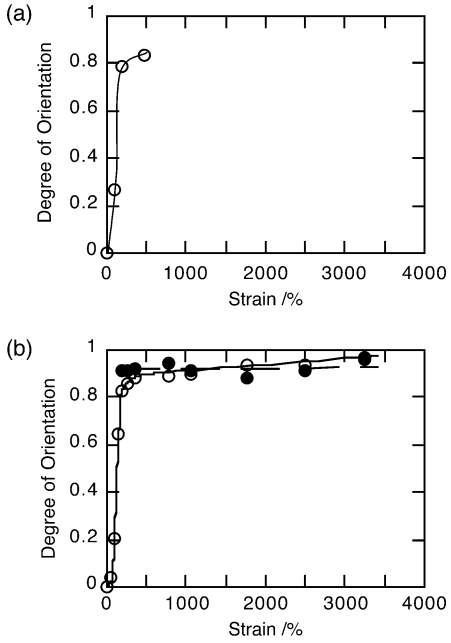

Figure 3. Variation of degree of layer orientation with strain, which was evaluated from WAXD profiles of smectic layer reflection: (a) at a strain rate of 5%/min at 60 °C and (b) at a strain rate of 100%/min at 60 °C. The open and closed circles represent the data points for the perpendicular and parallel orientations, respectively.

The degree of layer orientation

$$\langle P_2 \rangle = (3\langle \cos^2 \beta \rangle - 1)/2 \tag{1}$$

can be estimated from the intensity distribution $I(\beta)$ of layer reflection along the azimuthal angle (β) which is taken from the meridian according to the following equation:[16]

$$\langle \cos^2 \beta \rangle = \frac{\int_0^{\pi/2} I(\beta) \cos^2 \beta |\sin \beta| \, d\beta}{\int_0^{\pi/2} I(\beta) |\sin \beta| \, d\beta} \tag{2}$$

Here, $\langle P_2 \rangle = 1$ indicates the perfect orientation of the smectic layer with respect to the tensile direction and $\langle P_2 \rangle = 0$ indicates a random orientation. Figure 3a shows the variation of $\langle P_2 \rangle$ with strain. The $\langle P_2 \rangle$ value increases from 0 to 0.8 at the initial stage of elongation up to 200% and reaches 0.83 before breaking at 400% strain. Such a unique orientation with the polymer chains lying perpendicular to the elongation (or flowing) direction has also been observed in the rheology measurement for the series of main-chain BB-*n* type semiflexible polymers as well as the rigid-rod polymers.[15,17−23]

b. Deformation Process at High Strain Rate of 100%/min. Figure 4a−d shows the X-ray patterns observed for the films elongated at 100%/min and 60 °C. Figure 4a shows the X-ray pattern of the 50% strained film before the necking starts. It is found that the pattern is similar to that shown in Figure 2b. Thus, the perpendicular alignment is initially produced at a high strain rate as well. Interesting is that the X-ray pattern is markedly changed by the necking which starts at around 100% strain. As found in Figure 4b, smectic layer reflections appear on the equator as well as on the meridian, being well separated into four spots.[17−19] This indicates that some parts of the smectic layers are rearranged to lie perpendicular to the elonga-

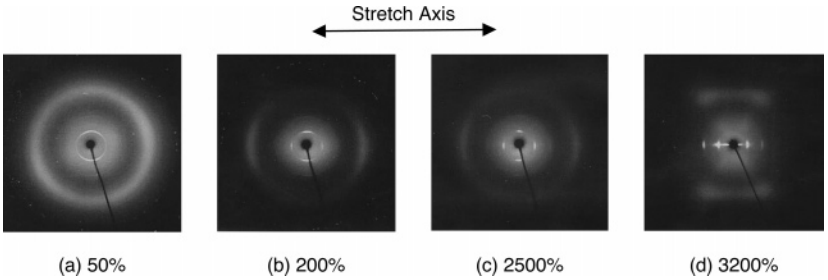

Figure 4. WAXD photographs of variously strained samples elongated at a rate of 100%/min at 60 °C: (a) 50% (before necking takes place), (b) 200% (at necked place), (c) 2500%, and (d) 3200%. The elongation direction is horizontal.

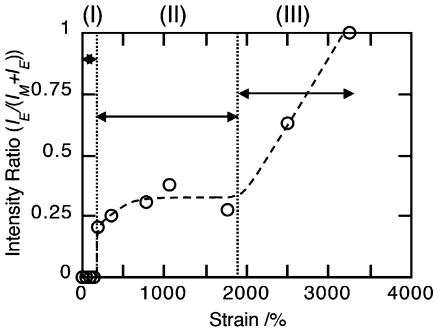

Figure 5. Variation of R with the strain for the samples strained at a rate of 100%/min at 60 °C. $R = 0$ and 1 indicate the perfect perpendicular and parallel orientations, respectively. In the strain region from 200% to 1800%, R is estimated for the necking part.

tion direction; i.e., the polymer main chains align parallel to the tensile axis (so-called "parallel orientation").

From an azimuthal scan of the layer reflections, the relative content of the molecules in the parallel alignment was estimated from a formula of $R = I_e/(I_e + I_m)$ in which I_e corresponds to the peak area of reflection appearing in an equatorial direction and I_m to the area of the reflection in the meridional direction.[24] $R = 0$ for the perpendicular orientation, and $R = 1$ for the parallel orientation. R is plotted against the strain in Figure 5. The variation of R with strain is very similar to that of stress with strain presented in Figure 1b. Again, the deformation process can be divided into three regions. In the first strain region from 0 to 100%, $R = 0$; that is, only the perpendicular orientation is observed. R increases abruptly up to 0.3 at around 200% strain by necking. Then, R at the necking part becomes again independent of the strain in the second region from 200% to 1800%, which corresponds to the plateau region of the $S-S$ curve where the necking deformation expands into the entire region of the film. We thus know that the necking results from the alteration of the perpendicular to the parallel orientation. In the third region from 1800% to 3200%, the continuous alteration takes place, and consequently, the parallel orientation becomes dominant just before breaking (see Figure 4c,d). This region corresponds to the final increment of stress in the $S-S$ curve.

The degree of orientation for both the perpendicular and parallel molecular alignments was also estimated using eqs 1 and 2 and plotted against the strain in Figure 3b. For the perpendicularly oriented molecules, as shown by the open circles in Figure 3b, the orientational degree increases from 0 to 0.85 with the increase in strain from 0 to 200%. Then it increases slightly with strain and finally reaches a high value of 0.95. On the other hand, the parallel orientation already has a high

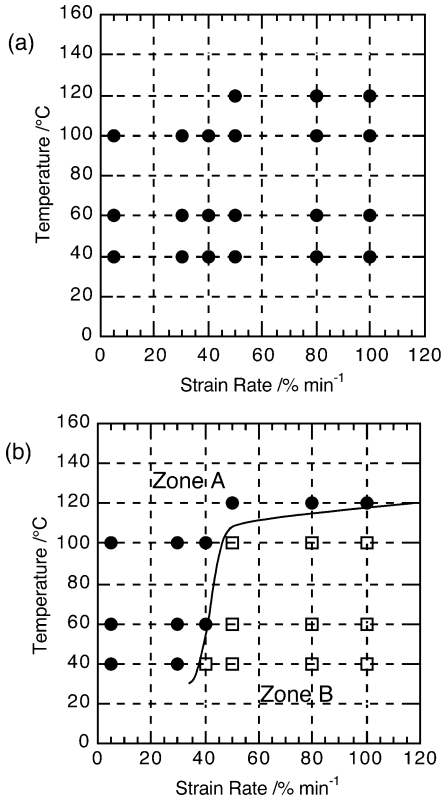

Figure 6. Strain rate−temperature diagram describing the molecular orientation observed in the strained smectic phase (a) with 100% strain and (b) at a breaking point. Closed circle and open square symbols represent the perpendicular and parallel orientations, respectively.

value of 0.92 when appearing first in accompanying the necking deformation, and its value stays constant with strain as presented by closed circles in Figure 3b. With the alteration of orientation, the intermediate states such as the oblique alignment state do not exist; molecules change their orientation from the perpendicular mode to the parallel mode in a flip-flop manner similarly to those in the Frederiks transition.[25] Similar features are also observed in the deformation of polyethylene crystal as cold drawing,[26,27] where the orientational exchange has been explained such that the arranged chain-folded lamellar crystals break and chains rearrange along the flow of elongation.

Dependence of Molecular Orientation on Temperature and Strain Rate. Figure 6a shows the orientation manner, perpendicular or parallel orientation, which is observed at a strain of 100% (just after the yielding point) as a function of temperature and strain rate. At any temperature and strain rate, the perpendicular orientation is invariably observed; in other words, no parallel orientation is observed in this

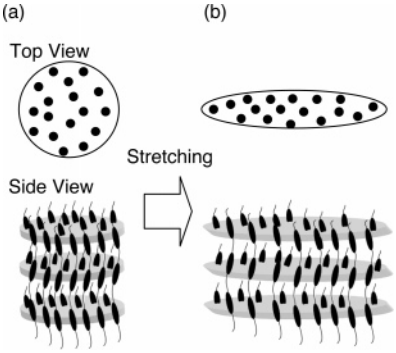

Figure 7. Schematic illustration of elongation deformation initiated in process A. When the smectic melt in (a) is stretched, the deformation is followed by the flow of molecules within a layer, resulting in the perpendicular orientation of molecules to the stretching direction as illustrated in (b).

strain range. Figure 6b shows the temperature and strain rate dependences of the orientation manner at the breaking point. In this case, the slower rates produce the perpendicular orientation (zone A) and the faster rates produce the parallel orientation (zone B) in the temperature range below 100 °C. However, at the high temperature of 120 °C, which is close to T_i, the perpendicular orientation is observed invariably with strain rate.

Temperature and time are synonymous. These dependences suggest that the molecular motion or relaxation in the system decides the orientation manner. Molecules can relax an applied stress at higher temperatures while they cannot do so at lower temperatures. Identically, when the deformation rate is slower than the intrinsic molecular motion, molecules can relax and dispense the applied stress, while they cannot relax the stress in high-rate deformation.

Discussion

Two Possible Deformation Mechanisms for Perpendicular Orientation Observed at Initial Stage of Strain. Typical flow of mesogens by elongation is observed in the nematic liquid crystals. Since the nematic liquid crystals possess only the orientational order, elongation simply results in the parallel-type orientation with the rodlike molecules lying parallel to the elongation direction. The present study, on the other hand, indicates that the elongation of smectic melt at the initial strain stage produces the perpendicular orientation independently of the elongation rate and temperature (see Figure 6a). This anomalous orientation is attributable to the structural nature of the smectic phase, and two possible mechanisms are considered.

The smectic CA phase treated here is the fluid layered phase where the mesogens' centers of mass have a one-dimensional layer order along the director but are isotropically distributed within a smectic layer, as illustrated in Figure 7a. That is, the rodlike chains, even if they are polymers, can move freely along the layer, i.e., in a perpendicular direction to their long axes.[11,15] Thus, the stretching is preferentially followed by the liquid flow of mesogens as shown in Figure 7b, when the deformation rate is relatively slower comparing to the intrinsic molecular motion (strain rate < (relaxation time)$^{-1}$) or when the temperature is relatively higher. This is the first possible process (process A) to result in the perpendicular orientation of molecules.

At the lower temperature and the higher strain rate where the internal flow of molecules within a layer is restricted, how does the smectic melt respond to the applied stress to produce the perpendicular orientation? A possible mechanism is the mutual slide of the smectic layer. In the smectic phase of the low-molecular-weight system, each smectic layer is constructed by individual molecules so that the smectic layers can slide from each other. In the polymeric smectic phase with the polymer chains running through several smectic layers, the mutual slide may take place between the chain-folded lamellae, as mentioned in Introduction and shown in Figure 8a. This is the second process (process B) to produce the perpendicular alignment. Although there is no way to distinguish these two types of mechanism in simple elongated samples, our previous study on steady shear deformation induced by the cone−plate-type rheometer has clearly shown these two mechanisms.[13]

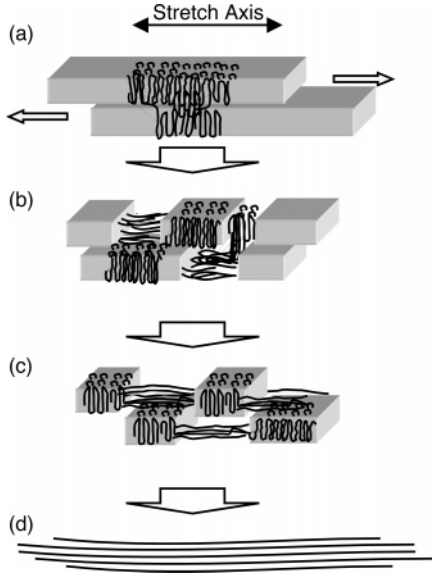

Figure 8. Schematic illustration of elongation deformation initiated in process B. In the initial stage, the deformation takes place with the mutual sliding of the chain folded lamellae, resulting in the perpendicular orientation of molecules (in (a)). On further elongation, the tie chains connecting the lamellae slip out from the lamellae and then align parallel to the elongation direction (in (b)). The sample is still elongated by unfolding of the residual lamellae (in (c)), and finally all chains align in the stretching direction before breaking (in (d)).

Deformation Mechanisms on Succeeding Elongation. The two deformation processes A and B at the initial stage may reflect in the different styles of the succeeding deformation which are classified into zones A and B in Figure 6b. At first, under the condition where the deformation is initiated by the internal flow of molecules within a layer (process A), the deformation becomes limited on further elongation because of the limited internal flow and the sample breaks at around 400% after completing the perpendicular orientation (see Figure 7). On the other hand, in the deformation initiated by the process B, mutual sliding of the lamellae is also limited on further elongation, but tie chains connecting the lamellae can conduct the stress from layer to layer. Then, they are split out from the lamellae to align along the tensile direction. As illustrated in Figure 8b, this deformation is attributed to the macroscopically observed necking, leading to a high elongation of up to 3000% by complete alteration of the perpendicular to parallel orientation (refer to Figure 8c,d).

Conclusions

Two distinct types of orientation process are observed depending on strain rate and temperature on the uniaxial elongation of smectic CA melt and are explained as a result of the balance between deformation rate and molecular relaxation time. When molecules can relax tensile stress by the flowing of chains within a smectic layer (process A), the mesogenic groups orient perpendicular to the tensile axis. In contrast, chain-folded lamellae orient along the tensile direction by their mutual sliding when they cannot relax the stress within layers (process B). Irrespective of the essential difference in deformation mechanism, both produce similar "perpendicular orientation". On further elongation, the difference in the deformation behavior between processes A and B becomes clear. When the deformation is initiated by process A, the sample is easily broken at the limited strain of around 400% because of the fluidity of molecules within a smectic layer. On the other hand, the deformation initiated by the process B is followed by the unfolding of chains from the chain-folded lamellae, which leads to a large deformation of the sample up to 3000%. The study, thus, clarifies the characteristic orientation behavior of polymeric smectic melt, which is completely different from that of conventional nematic melt.

References and Notes

(1) de Gennes, P. G. In *Polymer Liquid Crystals*; Cifferri, A., Krigbaum, W. R., Mayer, R. B., Eds.; Academic Press: New York, 1982; p 124.
(2) Wang, X. J.; Warner, M. *J. Phys., A* **1986**, *19*, 2215−2227.
(3) Williams, D. R. M.; Warner, M. *J. Phys. (Paris)* **1990**, *51*, 317−339.
(4) Li, M. H.; Brulet, A.; Davidson, P.; Keller, P.; Cotton, J. P. *Phys. Rev. Lett.* **1993**, *70*, 2297−2300.
(5) Li, M. H.; Brulet, A.; Cotton, J. P.; Davidson, P.; Strazielle, C.; Keller, P. *J. Phys. II* **1994**, *4*, 1843−1863.
(6) Krigbaum, W. R.; Watanabe, J. *Polymer* **1983**, *24*, 1299−1307.
(7) Tokita, M.; Takahashi, T.; Hayashi, M.; Inomata, K.; Watanabe, J. *Macromolecules* **1996**, *29*, 1345−1348.
(8) Tokita, M.; Osada, K.; Watanabe, J. *Liq. Cryst.* **1997**, *23*, 453−456.
(9) Tokita, M.; Osada, K.; Watanabe, J.; Yamada, M. *Macromolecules* **1998**, *31*, 24, 8590−8594.
(10) Takahashi, T.; Nagata, F. *Macromol. Sci. Phys.* **1989**, *B28*, C349−364.
(11) Tokita, M.; Osada, K.; Watanabe, J. *Polym. J.* **1998**, *30*, 589−595.
(12) Tokita, M.; Osada, K.; Kawauchi, S.; Watanabe, J. *Polym. J.* **1998**, *30*, 687−690.
(13) Tokita, M.; Tokunaga, K.; Funaoka, S.; Osada, K.; Watanabe, J. *Macromolecules* **2004**, *37*, 2527−2531.
(14) Hamley, I. W. *J. Phys.: Condens. Matter* **2001**, *13*, R643−R671.
(15) Osada, K.; Koike, M.; Tagawa, H.; Tokita, M.; Watanabe, J. *Macromol. Chem. Phys.* **2004**, *205*, 1051−1057.
(16) Mitchell, G. R.; Windle, A. H. In *Developments in Crystalline Polymers*; Bassett, D. C., Ed.; Elsevier: London, 1988; Vol. 2.
(17) Bello, P.; Bello, A.; Riande, E.; Heaton, N. J. *Macromolecules* **2001**, *34*, 181−186.
(18) Bello, P.; Bello, A.; Lorenzo, V. *Polymer* **2001**, *42*, 4449−4452.
(19) Martinez-Comez, A.; Perena, J. M.; Lorenzo, V.; Bello, A.; Perez, E. *Macromolecules* **2003**, *36*, 5798−5803.
(20) Alt, D. J.; Hudson, S. D.; Fujishiro, K. *Macromolecules* **1995**, *28*, 1575−1579.
(21) Romo-Uribe, A.; Windle, A. H. *Macromolecules* **1996**, *29*, 6246−6255.
(22) Leland, M.; Wu, Z.; Chhajer, M.; Ho, R. M.; Cheng, S. Z. D.; Kellar, A.; Kricheldorf, H. R. *Macromolecules* **1997**, *30*, 5249−5254.
(23) Zhou, W.; Kornfield, J. A.; Ugaz, V. M.; Burghardt, W. R.; Link, D. R.; Clark, N. A. *Macromolecules* **1999**, *32*, 5581−5593.
(24) It should be noted that R does not correspond to the real content of molecules in the parallel alignment since both I_e and I_m are proportional to the number of layers but with the different proportional constants in the present geometry.
(25) Sheng, P. In *Introduction to Liquid Crystals*; Priestly, E. B., Wojtowicz, P. J., Sheng, P., Eds.; Plenum: London, 1975; Chapter 8.
(26) Peterlin, A.; Meinel, G. *Makromol. Chem.* **1971**, *142*, 3536, 227−240.
(27) Peterlin, A. *Polym. Eng. Sci.* **1979**, *19*, 2, 118−124.

MA050649U